Scientific paper

Salt-Specific Effects in Solutions of Human Serum Albumin: Small-Angle X-Ray Scattering and Osmometry

Jaka Marušič, Jurij Reščič, Andrej Jamnik and Matija Tomšič*

University of Ljubljana, Faculty of Chemistry and Chemical Technology, Aškerčeva 5, SI-1000 Ljubljana, Slovenia

** Corresponding author: E-mail: Matija.Tomsic@fkkt.uni-lj.si*

Received: 13-11-2008

Dedicated to Professor Josef Barthel on the occasion of his 80th birthday

Abstract

Small-angle X-ray scattering (SAXS) method and membrane osmometry were used to study salt-specific effects of various 1:1 salts at pH 4.0 and 8.0 on interparticle interactions and thermodynamic quantities in aqueous solutions of human serum albumin (HSA) at 25 °C. Our results show that Donnan pressures of HSA solutions exhibit stronger dependence on the type of anion than on the type of cation in the solution. However, the presence of different salts in the HSA solutions only weakly affects the SAXS curves in the accessible q regime ($0.1\ nm^{-1} < q < 7\ nm^{-1}$). SAXS data were analyzed utilizing generalized indirect Fourier transformation, which indicated weak repulsive interactions between HSA molecules in all cases. Further, this analysis of the experimental SAXS curves strongly suggests that HSA molecules in the studied solutions have the shape of oblate ellipsoid with dimensions of approximately $8.5 \times 8.5 \times 4$ nm. Both SAXS and membrane osmometry results can be satisfactorily explained in terms of the strength of the inter-particle interactions and conform to the trends of the Hofmeister series.

Keywords: Human serum albumin, osmotic coefficient, small-angle X-ray scattering, indirect fourier transformation, Hofmeister series.

1. Introduction

Aqueous solutions of proteins are of substantial importance for the biological sciences as well as for related technologies. Separation of proteins from mixtures and their purification are among the most important techniques which require a detailed knowledge of protein behavior in aqueous solutions. At the molecular level of description, aqueous protein solutions are multicomponent systems that contain protein molecules, low molecular weight electrolyte, and water, and display a complex behavior, which is still far from being completely understood. Namely, thermodynamic properties of protein solutions at usual experimental conditions (pH, concentration and type of added electrolyte) notably differ from the ideal behavior.[1,2] Understanding the behavior of protein in these systems requires knowledge of the principal forces acting between the protein molecules;[1,3,4] these forces are modulated by the presence of a multi-component solvent. The interaction between protein molecules can be investigated by X-ray, neutron and light scattering, by hydrodynamic methods or by studying colligative properties of the solutions. Among the latter, Donnan pressure measurements are an important traditional source of information about protein-protein interactions.[5–7]

Despite being discovered already back in 1888 by Franz Hofmeister, the salt-specific effects are still an intriguing topic of modern reserch.[8,9] In the present work we use small-angle X-ray scattering (SAXS) and osmometry experimental techniques to study salt-specific effects in the human serum albumin (HSA) solutions with 0.15 M simple salt. The former method is well suited to reveal the correlations between the HSA molecules in solution and also their geometry (size and shape), whereas the Donnan pressure results provide information on the activity of simple salt in these systems. The goal of this paper is to mutually complement and discuss the results of the two methods and to check if the trends of the Hofmeister series are followed in the studied HSA solutions.

2. Experimental and Methods

2. 1. Materials

Salts NaCl, NaH_2PO_4, NaSCN, $NaNO_3$, LiCl, KCl, CsCl were purchased from Merck (Darmstadt, Germany), NaBr from Kemika (Zagreb, Croatia) and NaAc from Fluka. Human serum (HSA) was also obtained from Fluka, 05420, lot 131971445106137. To remove water from the initial substances the salts were dried in a vacuum drier at 120 °C for 2 hours and the HSA was dried at 40 °C for 24 hours in the presence of P_2O_5. The molar mass of HSA is around 67000 g/mol, slightly depending on the isolation procedure. All solutions were prepared gravimetrically, i.e. a weighted amount of HSA was dissolved in a weighted amount of 0.15 M solution of an individual salt. The HSA solutions from approximately 5 g/L to approximately 85 g/L have been prepared for the osmometry measurements. Solutions with 20 g/L of HSA were taken for the SAXS measurements. The pH of HSA solutions were adjusted to 4.0 or 8.0 with a small amount of appropriate acid or base. The choice of acid or base type was such that ion composition of the HSA solution remained the same, for example, KOH and HCl were used when the salt was KCl. The pH was measured by Iskra MA5740 pH meter (Ljubljana, Slovenia), using a combined glass microelectrode InLab 423 from Mettler Toledo (Columbus, OH). The iso-electric point of HSA is at pH around 5.4.

2. 2. Osmotic Pressure Measurements

Pressure difference established between the salt solution containing protein molecules and the salt solution without the protein is known as the Donnan pressure. The solutions are separated by a semi-permeable membrane that allows small ions and solvent to travel between the compartments but prevents protein molecules to diffuse into the protein-free solution. When the equilibrium is established across the membrane the electro-chemical potential $\bar{\mu}_i$ of all charged species but protein must be the same in compartments α and β, as well as the chemical potential of solvent μ_w:

$$\begin{aligned} &\mu_i^{0,(\alpha)} + kT \ln a_i^{(\alpha)} + z_i e_0 \Psi^{(\alpha)} = \\ &= \mu_i^{0,(\beta)} + kT \ln a_i^{(\beta)} + z_i e_0 \Psi^{(\beta)} \\ &\mu_w^{(\alpha)} = \mu_w^{(\beta)} \end{aligned} \quad (1)$$

Proteins are polyampholytes, i.e. molecules being able to possess both positive and negative charges simultaneously, and can be treated as weak polyelectrolytes. In the recent years several attempts have been made to treat such systems theoretically.[10–12] Assuming that activity coefficients of the solvent in both compartments are nearly equal, as well as that the activity coefficients of small ions are nearly the same, the following approximate equation can be derived:[13]

$$\Pi = RT\rho\phi \quad m_p + \frac{(Z_{net} m_p)^2}{4 m_{salt}} \quad (2)$$

where Π is Donnan pressure, R gas constant, T absolute temperature, ρ density of water, ϕ osmotic coefficient, m_p molality of protein, and m_{salt} molality of buffer. Eq. 2 provides a useful tool for obtaining the osmotic coefficients of protein solutions and the protein net charge Z_{net}.

To quantitatively compare the effect of various salts on the interactions between protein molecules, an equation:[14]

$$\frac{\Pi}{\Pi_{id}} = \phi = \frac{n_1}{n_2} \ln a_w \quad (3)$$

which correlates osmotic pressure Π to the activity of the solvent a_w, and the Gibbs-Duhem equation:[15]

$$d \ln a_w = \frac{n_2}{n_1} d \ln a_2 \quad (4)$$

were combined to yield the relation between the Donnan pressure Π and the activity of added salt a_2, assuming constant composition of the solution:

$$d \ln a_2 \propto d\Pi . \quad (5)$$

In these equations Π_{id} stands for ideal osmotic pressure, $\Pi_{id} = cRT$, n_1 for amount of solvent and n_2 amount of solute in moles. Eq. 5 shows that higher Donnan pressure reflects higher activity of the small ions in the solution. One of possible reasons for higher activity of the small ions could be weaker forces between small ions and protein molecules, which would in turn result in stronger repulsion between the protein molecules. Thus, one would expect that stronger repulsive forces between the protein molecules lead to higher Donnan pressure. However, one has to bear in mind that the level of hydration of small ions also influences their activity.

Osmotic pressure measurements were performed using Knauer membrane osmometer model 73101 (Berlin, Germany). Cellulose-acetate membranes with a cutoff of 12 kDa were used. The osmometer allows for maximum pressures of 4000 Pa. After mounting the membrane, the osmometer was left for baseline stabilization over the night. Typical measurement time for individual protein solution was 45 minutes.

2. 3. Small-Angle X-Ray Scattering Measurements

Small-Angle X-Ray Scattering (SAXS) spectra were measured with the Kratky compact camera (Anton Paar KG, Graz, Austria),[16] which was attached to a conventional X-ray generator Kristalloflex 760 (Bruker AXS GmbH, Karlsruhe, Germany) equipped with a sealed X-ray tu-

be (Cu K_α X-rays with a wavelength $\lambda = 0.154$ nm) and operating at 35 kV and 35 mA. 10 μm thick Ni foil was used as a filter for primary X-ray beam, which eliminated a large portion of Cu K_β line – a large portion of Cu K_α line, which was of interest for the scattering, was still transmitted. In addition a software monochromator was also used, which considered only the scattered X-ray photons within a predefined window of energies and in this way eliminated also hard X-rays from the detected scattered light. The samples were measured in a standard quartz capillary with an outer diameter of 1 mm and wall thickness of 10 μm. The scattered X-ray intensities were detected with the position sensitive detector PSD ASA (M. Braun GmbH, Garching, Germany) in the small-angle regime of scattering vectors $0.1 < q < 7$ nm^{-1}, where $q = 4\pi/\lambda \cdot \sin(\vartheta/2)$, ϑ being the scattering angle. The measuring times of 20 hours yielded sufficient measuring statistic. Scattering data were corrected for the empty capillary and solvent scattering, put on absolute scale using water as a secondary standard[17] and were subsequently further normalized to the scattering at large angles in order to easier observe small differences in SAXS curves at low q values. SAXS intensities obtained in this way were therefore not exactly on the absolute scale and are consequently given in arbitrary units. Furthermore, they are also still experimentally smeared because of the finite dimensions of the primary Beam.[18]

2. 4. Indirect Fourier Transformation of SAXS Data

Experimental SAXS curves were analyzed with the Generalized Indirect Fourier Transformation GIFT[19–24] which is an extension of the Indirect Fourier Transformation method IFT.[25–27] The latter is a model-free method appropriate only for dilute particulate systems with negligible interparticle interactions; for higher concentrations its generalized version with the modeled interparticle interactions has to be used. GIFT is based on the assumption that the scattering intensity $I(q)$ can be represented as a product of the form factor $P(q)$ and the structure factor $S(q)$:[23]

$$I(q) = n \cdot P(q) \cdot S(q), \tag{6}$$

where n is the number density of scattering particles. Form factor represents the intra-particle scattering contributions and can be written as the Fourier transformation of the pair-distance distribution function $p(r)$:[25,26]

$$P(q) = 4\pi \int_0^\infty p(r) \frac{\sin(qr)}{qr} dr, \tag{7}$$

where r is the distance between two scattering centers within the particle. Pair-distance distribution function serves as a tool for the determination of the scattering particles' geometry.[23,28] At distances r bigger than the maximum dimension of particle the $p(r)$ function adopts the value of zero and in this way provides a useful tool for determination of the particle's maximum dimension. Further, from the shape of this function the type of scattering particles' symmetry can be deduced. Structure factor $S(q)$ is important in the case of considerable interparticle interactions, when it significantly contributes to the total scattered intensity. In the real (r) space inter-particle interactions can be described via the total correlation function $h(r) = g(r)$-1, with $g(r)$ being the radial distribution function and r the distance between the centres of particles.[29] Similarly to the connection between $P(q)$ and $p(r)$ through Eq. 7, also $S(q)$ and $h(r)$ form the Fourier transform pair:

$$S(q) = 1 + 4\pi n \int_0^\infty h(r) r^2 \frac{\sin(qr)}{qr} dr. \tag{8}$$

Various models and methods are incorporated in the GIFT software package offering the use of appropriate structure factor $S(q)$. In the present study we were especially interested in the interparticle interactions between the HSA molecules and in their effect on the SAXS spectra, therefore the interparticle interactions had to be considered very carefully. For this reason a rather complex model of monodisperse charged hard-spheres with Yukawa potential and Rogers-Young (RY)[30] closure relation was used. The latter approximation represents a combination of the Percus–Yevick[31] closure relation that works well for short-ranged interactions and hypernetted chain (HNC) closure relation, which performs the best for systems with long-ranged (usually electrostatic) interactions.[22] RY closure relation is designed to treat strongly correlated systems with repulsively interacting particles. For this reason, it is a good choice for the study of inter-particle correlations in the case of highly charged HSA particles screened by the presence of ions of simple salts. In the GIFT procedure the RY structure factor model is described by two parameters, i.e., concentration of salt and the dielectric constant of the solvent, which are kept fixed, and additional three parameters, i.e., volume fraction φ, radius R, and effective charge Z_{eff} of the scattering particles, which can be varied during the evaluation.[22] Due to the strong correlation between the parameters φ, R, and Z_{eff}, one of them is usually also fixed during the evaluation in order to get physically reasonable values for the remaining two parameters.[22] However, due to the high concentration of simple salt in the studied HSA samples interparticle interactions turned out to be substantially screened; therefore they were only weakly expressed in the SAXS curves leading to the necessity to fix one additional parameter of the structure factor. Correspondingly, we chose to fix the radius (R = 4.25 nm was selected according to the resulting $p(r)$ function) and volume fraction ($\varphi = 0.02$ was a reasonable guess obtained according to the sample composition). Consequently the effective charge Z_{eff} was the only remaining parameter of the structure factor that was actually varied du-

ring the evaluation of SAXS data, therefore all the differences between the individual $S(q)$ were fully reflected in the resulting value of this parameter. Furthermore, the effective charge Z_{eff} anyway represents a rescaled charge of the scattering particle and therefore has less physical meaning.[32] The latter fact is, however, not only the consequence of the definition of Z_{eff} but also the consequence of the evaluation procedure itself. Nevertheless, the form factor $P(q)$ and the corresponding $p(q)$ function, which are considered as the model-free results, are usually successfully determined in such GIFT evaluation of the SAXS curves. Namely, utilizing the simulated data it has been also shown that the interparticle interactions are usually approximated rather well even in the case of the unphysical resulting values of structure factor parameters, and that the evaluation still leads to the correct results for the form factor $P(q)$ and pair distance distribution function $p(r)$.[22]

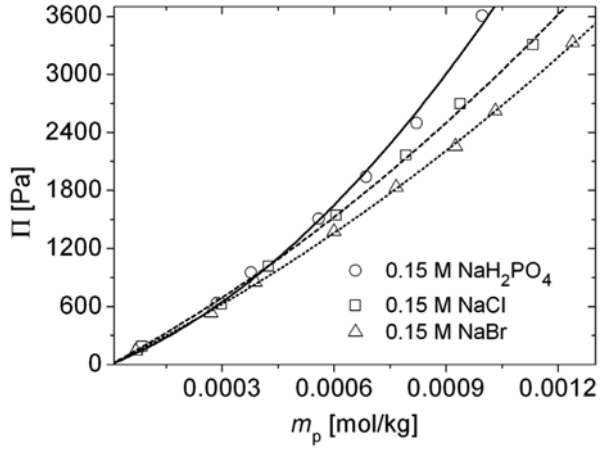

Figure 1: The salt-specific effect of various anions on Donnan pressures of HSA solutions at pH 4.0. Filled symbols denote experimental data, whereas lines represent the fits according to Eq. 2.

3. Results and Discussion

3. 1. Osmotic Pressure

The Donnan pressure of HSA solutions was measured at two different pH values, 4.0 and 8.0. In order to obtain the protein's net charge Z_{net} and the osmotic coefficient ϕ of the solution Eq. 2. was fitted to the experimental data. The obtained results are represented in Table 1 with the corresponding experimental data and fits shown in Figure 1, Figure 2 and Figure 3. Examination of the collected results indicates that HSA molecules at pH 4.0 carry a net charge of about +15 e_0, whereas at pH 8.0 the net charge of the molecules is about –20 e_0. The iso-electric point of the HSA is at pH around 5.4, therefore such charge polarity reversal going from pH 4.0 to 8.0 is expected. The fitting procedure yields osmotic coefficient values in the range of 0.76–0.86; the result indicates substantial deviations from the ideal behavior.

Table 1: Net charge Z_{net} and osmotic coefficient ϕ of HSA solutions with various 0.15 M salts at pH values of 4.0 and 8.0 as resulting from the fits of data in Figures 1–3 according to Eq. 2.

pH	Salt	Z_{net}	ϕ
4	NaH_2PO_4	27	0.63
	NaCl	15	0.84
	NaBr	14	0.76
8	NaSCN	–21	0.85
	$NaNO_3$	–21	0.80
	NaCl	–20	0.82
	NaAc	–22	0.69
8	CsCl	–20	0.86
	NaCl	–20	0.82
	LiCl	–19	0.85

However, one has to note that Eq. 3 assigns a single value of the osmotic coefficient to a range of solutions with different HSA concentrations.

Figure 1 displays experimental data of sodium salt solutions of HSA at pH 4.0. Protein solutions which contain Br^- ions exhibit lower Donnan pressure than solutions containing Cl^- and $H_2PO_4^-$ ions. As explained in the Experimental and Methods section, larger Donnan pressure reflects larger activity of the small ions, which could be the consequence of weaker attraction between the protein molecules and small counterions. Accordingly, such behavior could speak in favor of stronger repulsive forces between HSA molecules. However, one has to be aware of the fact that due to a rather large molar ratio salt/HSA in the sample, the small ions are the actual species that contribute substantially to the colligative property such as osmotic activity – in this sense the small ions are the actual particles that build up the Donnan pressure. Of course, the HSA macromolecules cooperate in the overall Donnan equilibrium, but they influence Donnan pressure mainly indirectly by interacting with the small ions. Nevertheless, arranging anions into a series and beginning with the anion which is expected to induce the strongest repulsive interactions between HSA molecules, gives the following order: $H_2PO_4^- > Cl^- > Br^-$. The results for protein net charge presented in Table 1 are in very good agreement with the data available from the literature[33] with the only exception in the case of $H_2PO_4^-$. This net charge value is substantially larger than the other two at pH 4.0. Although this is a large deviation it could be at least partially explained by the influence of the size of hydrated anions. Similar explanation of the anion size effect was already used in the study of lysozyme solubility in polyethylene glycol-electrolyte mixtures.[34] Namely, the size of hydrated anions increases in order $Br^- < Cl^- < H_2PO_4^-$, with the $H_2PO_4^-$ anion correspondingly causing the weakest screening between the HSA molecules.

Similarly, the effect of anions on the behavior of protein solutions at pH 8.0 is shown in Figure 2. SCN^- ions exhibit the highest Donnan pressures and are therefore ex-

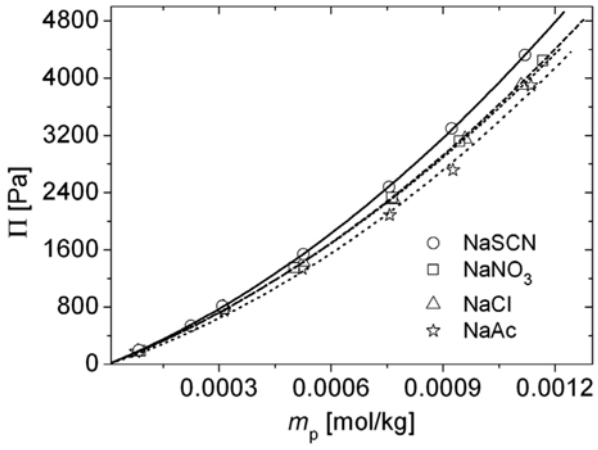

Figure 2: The effect of anions on Donnan pressures of HSA solutions at pH 8.0. Symbols denote experimental data, whereas lines represent the fit according to Eq. 2.

pected to induce the strongest repulsive interactions between HSA molecules. The series of anions at pH 8.0 is thus as follows: $SCN^- > NO_3^- > Cl^- > Ac^-$. It is evident that the trend of Donnan pressures shows the reversal in the anion sequence in respect to the Hofmeister series when changing from pH 4.0 to 8.0. It is also evident that the effect of anions on Donnan pressure is stronger at pH 4.0 where they act as counterions than at pH 8.0 where they act as coions of the protein. In this sense these results are the consequence of the charge polarity reversal of the HSA molecules with the increase in the pH from 4.0 to 8.0.

The influence of various cations on the Donnan pressure of HSA solutions is in general less pronounced than that of anions. The results of the Donnan pressure measurements for cation series at pH 8.0 are shown in Figure 3 and reveal the following order of cations with decreasing activity in the studied samples: $Cs^+ > Na^+ > Li^+$.

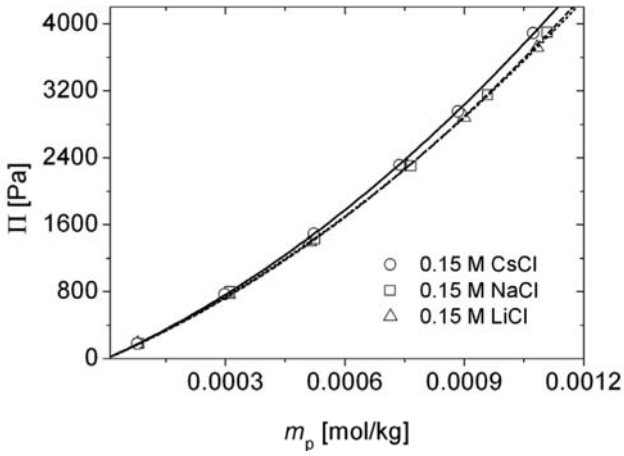

Figure 3: The effect of cations on Donnan pressures of HSA solutions at pH 8.0. Symbols denote experimental data whereas lines represent the fit according to Eq. 2.

3. 2. Small-Angle X-Ray Scattering Intensities

The results of the Donnan pressure measurements of the HSA solutions with various salts were complemented with the SAXS study of the same solutions. SAXS measurements were performed for the 20 g/L HSA samples ($m_p \approx 0.0003$ mol/kg) in 0.15 M salt solutions at pH 8.0 and are presented as anionic and cationic series in Figure 4. Already from the raw experimental SAXS data shown in Figure 4 one can observe that the scattering curves practically coincide from moderate q values on, while slight differences can be observed in the regime of small values of q. Such differences between the individual SAXS curves could be easily explained with the help of Eq. 6. Namely, if one assumes constant form factor of the scattering particles and increasing repulsive liquid-type interactions between them, such lowering of the SAXS intensity in the low q regime would be expected. However, due to Fourier transformation relating the real and reciprocal space quantities it is rather dangerous to interpret the raw SAXS data

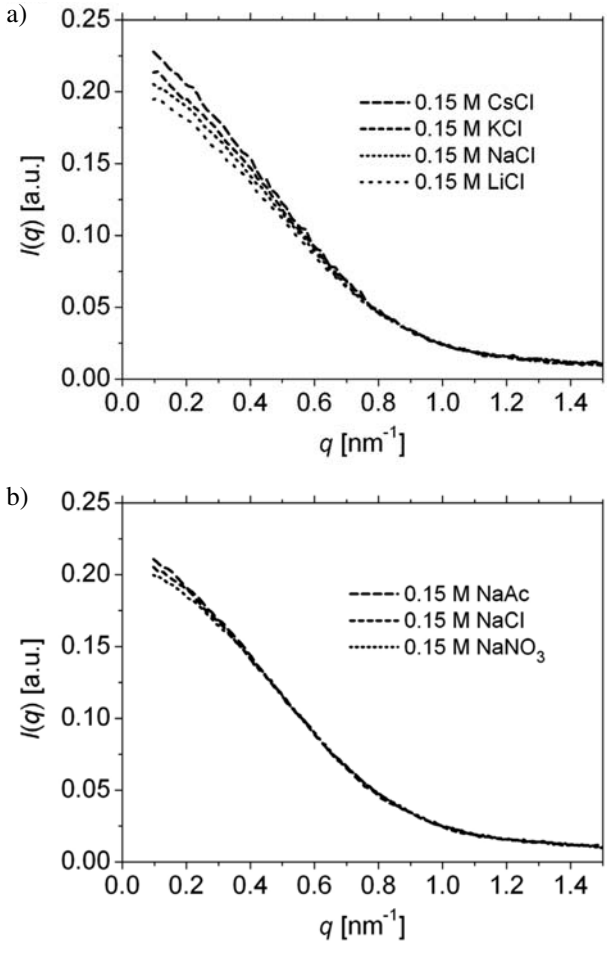

Figure 4: Experimental SAXS curves of 20 g/L HSA in various salt solutions at pH 8.0. The curves are normalized to coincide at large q values for the sake of clarity and are therefore on an arbitrary scale although very close to an absolute scale.

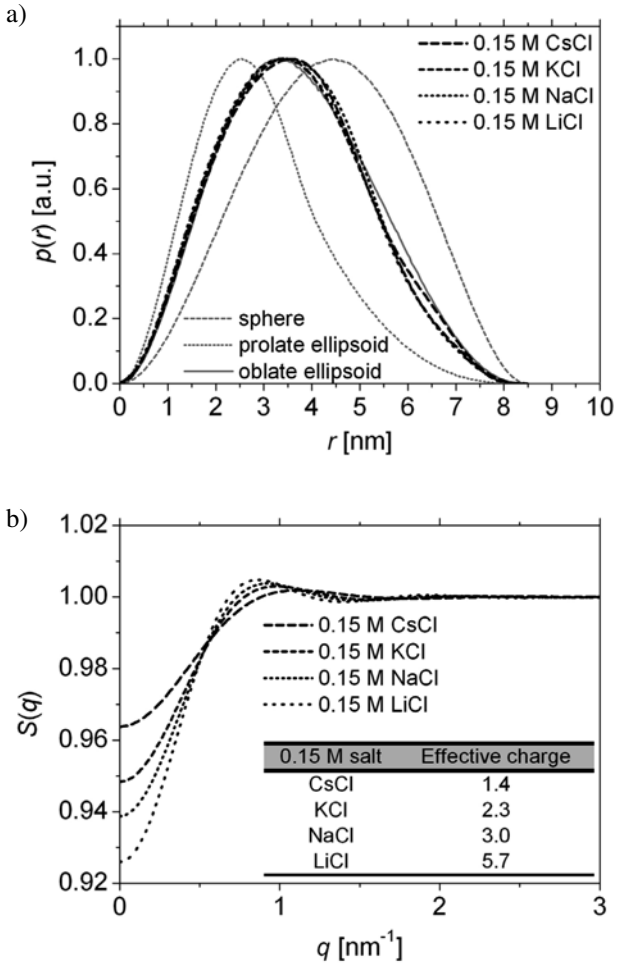

Figure 5: GIFT results of the experimental SAXS curves from Figure 4a – cation series. (a) Resulting model-free pair distance distribution functions $p(r)$ and (b) the corresponding modeled structure factor curves $S(q)$. Inset: resulting structure factor parameter values for the effective charge Z_{eff}. For the sake of clarity $p(r)$ functions are normalized to the same height.

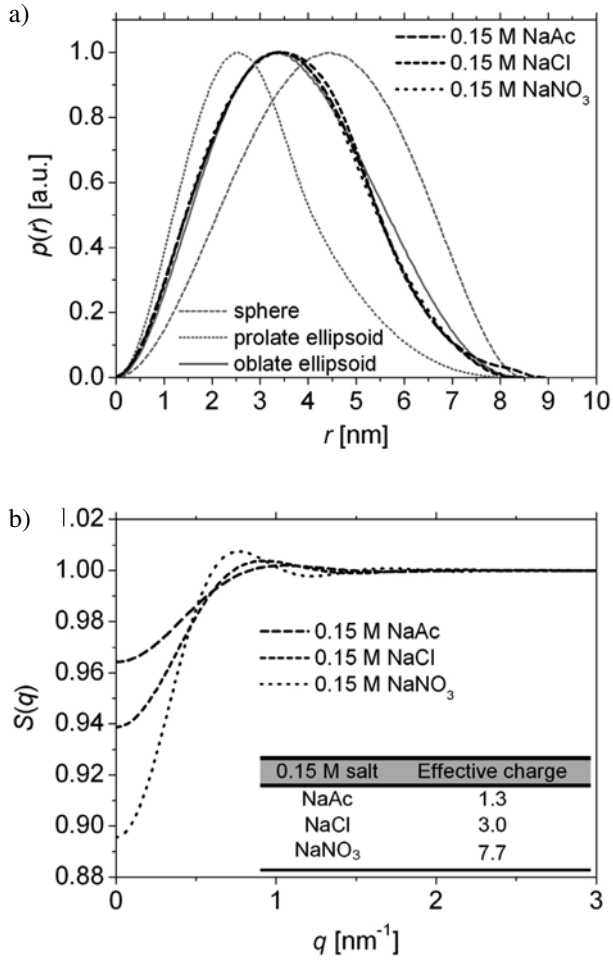

Figure 6: GIFT results of the experimental SAXS curves from Figure 4b – anion series. (a) Resulting pair distance distribution functions $p(r)$ and (b) the corresponding modeled structure factor curves $S(q)$. Inset: resulting structure factor parameter values for the effective charge Z_{eff}. For the sake of clarity $p(r)$ functions are normalized to the same height.

directly. Consequently, these data were interpreted utilizing the GIFT[19-24] evaluation technique. The results for the cationic and anionic series are depicted in Figure 5 and Figure 6, respectively. They are presented in a form of pair-distance distribution function $p(r)$, revealing the internal structure and geometry of scattering particles, and structure factor $S(q)$, representing the information on the interparticle interactions. The shape of the $p(r)$ functions in Figure 5a reveals that the scattering particles are homogeneous with maximal dimensions around 8.5 nm in all cases. This proves that the form factors $P(q)$ are indeed more or less constant in the studied samples and that the slight differences in the SAXS spectra from Figure 4 can be attributed solely to the differences in the interparticle interactions. Further, comparing the shapes of the resulting $p(r)$ functions (black lines) with those of the simulated $p(r)$ functions (grey lines) for a spherical particle with diameter D = 8.5 nm, prolate ellipsoid with semi-axes a = b = 2 nm and semi-axis c = 4.25 nm, and oblate ellipsoid with semi-axes a = b = 4.25 nm and semi-axis c = 2 nm clearly reveals nearly perfect match in the case of the oblate ellipsoid. The latter is thus the correct geometry of HSA molecules in these solutions. All these findings are also true for the results presented in Figure 6a. We can only briefly comment the shoulder observed in the $p(r)$ function of the sodium acetate sample, which is stretching a little further out than in other cases. We interpret it in a sense that the ionic cloud of the rather large acetate anions most probably develops a sufficient scattering contrast to be able to contribute to the form factor and apparently slightly increase the observed size of HSA molecules in this sample.

Inspecting further the structure factor results shown in Figure 5b and Figure 6b we can clearly observe an increasing repulsive interparticle interactions between the HSA molecules in the sequence $Cs^+ < K^+ < Na^+ < Li^+$ for

the varying cations and in the sequence $COOH^- < Cl^- < NO_3^-$ for the varying anions. These sequences conform to the Hofmeister series. For the case of anions a similar SAXS results have already been reported.[35] Interestingly, the sequence for anions agrees with the order obtained from the interpretation of the Donnan pressure measurements. However, the trend of expected interparticle repulsions between the HSA molecules obtained from the Donnan pressure results for varying cations seems to be just the opposite as the trend of interparticle interactions revealed by the SAXS results. At this point we have to stress that the interparticle interactions in the form of structure factor $S(q)$ are the actual direct result of the SAXS data interpretation. On the contrary, the Donnan pressure measurements directly reveal the trends in the change of the activity of the small ions, while the trend of expected repulsions between HSA molecules based on this activity changes is only a possible consequence. As can be seen in Figure 2 and Figure 3, it is also true that the Donnan pressures at this specific HSA concentration show larger differences in the case of anion series than in the case of cation series. Thus, some further studies of these cation series might be of interest to clarify some of these qualitative discrepancies between the results of both methods. In any case, the $S(q)$ curves in Figure 5b and Figure 6b reveal repulsive interparticle interactions in all cases. However, according to the $S(0)$ values these interparticle interactions are not very pronounced. This is a consequence of the strong screening effect of simple salts, which are added at rather high concentration. In comparison to the net charge of the HSA molecules obtained from Donnan pressure results the effective charge values seem to be rather low, but one has to bear in mind that the effective charge anyway represents a rescaled charge of the scattering particle and therefore has no clear physical meaning.[32]

Eventually, we have to comment the present findings on the HSA solutions in terms of our previous similar investigations.[2,36] Namely, we seem to obtain somewhat puzzling results for the actual geometry of the HSA molecules in solutions. It is true that we have used different batches of HSA for every individual study but all of them were purchased from the same company with the same lot number. Nevertheless, due to the fact that one can actually find different structures of HSA in the literature[2,36–40] we suspect that HSA in solutions is obviously rather tricky either in terms of stability or in terms of various possible conformations varying from oblate ellipsoid of maximal dimension about 8.5 nm to prolate ellipsoid of maximal dimension approximately 14 nm.

4. Conclusions

Thermodynamic properties of aqueous protein solutions are governed by complex interactions among all species in the solution. Both non-electrostatic and electrostatic forces contribute to the non-ideality of these solutions which was in our case clearly evidenced with the Donnan pressure results. With this investigation we were able to demonstrate that the effects of various simple salts on the Donnan equilibrium and small-angle X-ray scattering of HSA solutions follow the Hofmeister series. We interpreted the results in terms of different activities of the ions in solutions and different repulsive liquid-type interactions between the HSA molecules. We were also able to demonstrate that oblate ellipsoid with dimensions 8.5 × 8.5 × 4 nm is the correct geometry of HSA molecules in these solutions.

5. Acknowledgement

We would like to thank Prof. Vojko Vlachy for helpful discussions. We acknowledge the financial support of the Slovenian Research Agency through the Physical Chemistry Program Group P1-0201.

6. References

1. J. Wu, J. M. Prausnitz, *Fluid Phase Equil.* **1999**, *155*, 139–154.
2. J. Reščič, V. Vlachy, A. Jamnik, O. Glatter, *J. Colloid Interf. Sci.* **2001**, *239*, 49–57.
3. Y. U. Moon, R. A. Curtis, A. Anderson, H. W. Blanch, J. M. Prausnitz, *J. Solution Chem.* **2000**, *29*, 699–717.
4. F. W. Tavares, D. Bratko, H. W. Blanch, J. M. Prausnitz, *J. Phys. Chem. B* **2004**, *108*, 9228–9235.
5. V. L. Vilker, C. K. Colton, K. A. Smith, *J. Colloid Interf. Sci.* **1981**, *79*, 548–566.
6. C. A. Haynes, K. A. Tamura, R. H. Körfer, H. W. Blanch, J. M. Prausnitz, *J. Phys. Chem.* **1992**, *96*, 905–912.
7. K. M. Kanal, G. D. Fullerton, I. L. Cameron, *Biophys. J.* **1994**, *66*, 153–160.
8. W. Kunz, J. Henle, B. W. Ninham, *Curr. Opin. Coll. Interf. Sci.* **2004**, *9*, 19–37.
9. W. Kunz, P. Lo Nostro, B. W. Ninham, *Curr. Opin. Coll. Interf. Sci.* **2004**, *9*, 1–18.
10. V. Vlachy, J. M. Prausnitz, *J. Phys. Chem.* **1992**, *96*, 6465–6469.
11. M. Druchok, Y. V. Kalyuzhnyi, J. Reščič, V. Vlachy, *J. Chem. Phys.* **2006**, *124*, 114902.
12. F. Jiménez-Ángeles, M. Lozada-Cassou, *J. Phys. Chem. B* **2004**, *108*, 1719–1730.
13. H. Dautzenberg, W. Jaeger, J. Kötz, B. Philipp, C. Seidel, D. Stcsherbina Polyelectrolites: Formation, Characterisation and Application; Hanser: Munich, **1994**.
14. G. N. Lewis, M. Randall Thermodynamics, 2_{nd} ed.; McGraw-Hill Book Company, Editorial Novaro-Mexico, S.A.: Mexico, **1965**.
15. P. Atkins, J. de Paula Atkins' Physical Chemistry, 8^{th} ed.; Oxford University Press: Oxford, **2006**.

16. O. Kratky, H. Stabinger, *Colloid Polym. Sci.* **1984**, *262*, 345–360.
17. D. Orthaber, A. Bergmann, O. Glatter, *J. Appl. Crystallogr.* **2000**, *33*, 218–225.
18. O. Glatter, in: O. Glatter, O. Kratky (Eds.): Small angle x-ray scattering, Academic Press Inc. London Ltd., London, **1983**, pp. 119–165.
19. O. Glatter, *J. Appl. Crystallogr.* **1979**, *12*, 166–175.
20. B. Weyerich, J. Brunner-Popela, O. Glatter, *J. Appl. Crystallogr.* **1999**, *32*, 197–209.
21. J. Brunner-Popela, O. Glatter, *J. Chem. Phys.* **1999**, *110*, 10623–10632.
22. G. Fritz, A. Bergmann, O. Glatter, *J. Chem. Phys.* **2000**, *113*, 9733–9740.
23. O. Glatter, in: P. Lindner, T. Zemb (Eds.): Neutron, X-rays and Light: Scattering Methods Applied to Soft Condensed Matter, Elsevier, Amsterdam, **2002**.
24. G. Fritz, O. Glatter, *J. Phys.: Condens. Matter* **2006**, *18*, S2403–S2419.
25. O. Glatter, *Acta Phys. Austriaca* **1977**, *47*, 83–102.
26. O. Glatter, *J. Appl. Crystallogr.* **1977**, *10*, 415–421.
27. O. Glatter, *J. Appl. Crystallogr.* **1980**, *13*, 577–584.
28. O. Glatter, in: O. Glatter, O. Kratky (Eds.): Small Angle X-Ray Scattering, Academic Press Inc. London Ltd., London, **1983**, pp. 167–196.
29. J. P. Hansen, I. R. McDonald *The Theory of Simple Liquids*; Academic Press: London, 1990.
30. F. J. Rogers, D. A. Young, *Phys. Rev. A* **1984**, *30*, 999.
31. J. K. Percus, G. J. Yevick, *Phys. Rev.* **1958**, *110*, 1.
32. L. Belloni, *J. Chem. Phys.* **1986**, *85*, 1.
33. N. Fogh-Andersen, P. J. Bjerrum, O. Siggard-Andersen, *Clin. Chem.* **1993**, *39*, 48–52.
34. M. Bončina, J. Reščič, V. Vlachy, *Biophys. J.* **2008**, *95*, 1285–1294.
35. S. Finet, F. Skouri-Panet, M. Casselyn, F. Bonnete, A. Tardieu, *Curr. Opin. Coll. Interf. Sci.* **2004**, *9*, 112–116.
36. P. Zalar, M. Tomšič, A. Jamnik, J. Reščič, *Acta. Chim. Slov.* **2006**, *53*, 344–349.
37. B. Sjöberg, K. Mortensen, *Biophys. Chem.* **1994**, *52*, 131–138.
38. X. M. He, D. C. Carter, *Nature* **1992**, *358*, 209–215.
39. B. Sjöberg, K. Mortensen, *Biophys. Chem.* **1997**, *65*, 75–83.
40. M. A. Kiselev, Y. A. Gryzunov, G. E. Dobretsov, M. N. Komarova, *Biofizika* **2001**, *46*, 423–427.

Povzetek

S pomočjo metode ozkokotnega rentgenskega sipanja (SAXS) in membranske osmometrije smo raziskali specifične vplive različnih 1:1 soli na meddelčne interakcije in termodinamske količine vodnih raztopin človeškega serumskega albumina (HSA) pri 25 °C in pH 4.0 ter 8.0. Rezultati so pokazali, da je donnanski tlak takšnih HSA raztopin močneje odvisen do tipa aniona kot od tipa kationa soli v raztopini. Zanimivo pa je, da prisotnost različnih soli v HSA raztopinah le rahlo vpliva na eksperimentalne rezultate SAXS v dostopnem območju sipalnih vektorjev q ($0.1\ \mathrm{nm}^{-1} < q < 7\ \mathrm{nm}^{-1}$). Sipalne krivulje so bile ovrednotene s pomočjo posplošene indirektne Fourierove transformacije, ki je razkrila, da so v vseh raziskanih raztopinah interakcije med HSA molekulami odbojne. Pokazala je tudi, da so HSA molekule v teh raztopinah oblike oblatnega elipsoida z dimenzijami približno $8.5 \times 8.5 \times 4$ nm. Predstavljeni rezultati se skladajo s trendi Hofmeistrove vrste in so se dali tudi zadovoljivo dobro razložiti v smislu različnih jakosti meddelčnih interakcij.